



Assessment of railway vibrations using an efficient scoping model



D.P. Connolly^{a,*}, G. Kouroussis^b, A. Giannopoulos^c, O. Verlinden^b,
P.K. Woodward^a, M.C. Forde^c

^a Heriot-Watt University, Institute for Infrastructure & Environment, Edinburgh, UK

^b Department of Theoretical Mechanics, Dynamics and Vibrations, University of Mons, 31 Boulevard Dolez, B-7000 Mons, Belgium

^c University of Edinburgh, Institute for Infrastructure and Environment, School of Engineering, AGB Building, The Kings Buildings, Edinburgh, UK

ARTICLE INFO

Article history:

Received 6 November 2013

Received in revised form

10 December 2013

Accepted 13 December 2013

Available online 7 January 2014

Keywords:

High speed rail vibration

Environmental impact assessment

ScopeRail

High speed train

ABAQUS

Initial vibration assessment

High-speed ground transportation

Railway track dynamics

Scoping assessment

Free field

ABSTRACT

Vibration assessments are required for new railroad lines to determine the effect of vibrations on local communities. Low accuracy assessments can significantly increase future project costs in the form of further detailed assessment or unexpected vibration abatement measures.

This paper presents a new, high accuracy, initial assessment prediction tool for high speed lines. A key advantage of the new approach is that it is capable of including the effect of soil conditions in its calculation. This is novel because current scoping models ignore soil conditions, despite such characteristics being the most dominant factor in vibration propagation. The model also has zero run times thus allowing for the rapid assessment of vibration levels across rail networks.

First, the development of the new tool is outlined. It is founded upon using a fully validated three dimensional finite element model to generate synthetic vibration records for a wide range of soil types. These records are analysed using a machine learning approach to map relationships between soil conditions, train speed and vibration levels. Its performance is tested through the prediction of two independent international vibration metrics on four European high speed lines and it is found to have high prediction accuracy.

A key benefit from this increased prediction accuracy is that it potentially reduces the volume of detailed vibration analyses required for a new high speed train line. This avoids costly in-depth studies in the form of field experiments or large numerical models. Therefore the use of the new tool can result in cost savings.

© 2013 Elsevier Ltd. All rights reserved.

1. Introduction

High speed rail infrastructure is experiencing rapid international growth. This growth has led to a desire to construct new railway lines in urban environments. One side-effect of increased train speeds is that elevated levels of ground borne vibration can be generated. Therefore, if lines are constructed near sensitive buildings (e.g. hospitals) then it is possible that the primary functions of these buildings may be impaired. This is undesirable because expensive abatement methods (e.g. [3,14,15]) may be required to reduce these vibrations, or in extreme cases these buildings may need to be decommissioned. These concerns mean that during the planning stage of new high speed lines, it is common to undertake a vibration assessment study. These studies typically exist in two forms: preliminary and detailed. This work focuses on improving the accuracy of preliminary studies.

First, to perform an initial (aka preliminary or scoping) railway vibration assessment study, vast sections of track must be analysed in a short time frame, meaning the use of a prediction model with low computation requirements is vital. If a fully 3D model was used to perform such an analysis, the associated computer run times would be impractical for commercial use. Additionally, the number of inputs required to deploy a scoping model must be few and availability of these parameters must be high. Although a model may have high prediction accuracy and run quickly, if it requires highly detailed geotechnical information that is only obtainable through field experiments, then the physical collection of data becomes the limiting factor.

A scoping model was developed by the Norwegian Geotechnical Institute [23] to predict vibration levels in buildings close to railway lines. The model was based upon a statistical analysis of measured vibration levels at a variety of test sites in Norway and Sweden. It was used for predicting vibration levels on a high speed rail track between Oslo city and Oslo airport.

Bahrekazemi [2] presented an alternative empirical model to estimate one second r.m.s vibration values. Experimental work was undertaken to record railway vibration levels at four Swedish test sites (Kahog, Partille, Ledsgard and Sabylund). The results were used to develop a model that predicted vibration levels based upon train speed, receiver distance, vibration attenuation

* Corresponding author. Tel.: +44 131 451 8051.

E-mail addresses: d.connolly@hw.ac.uk (D.P. Connolly),
georges.kouroussis@umons.ac.be (G. Kouroussis),
a.giannopoulos@ed.ac.uk (A. Giannopoulos),
olivier.verlinden@umons.ac.be (O. Verlinden),
p.k.woodward@hw.ac.uk (P.K. Woodward), m.forde@ed.ac.uk (M.C. Forde).

and wheel force. The model was verified using data from the same four sites, which was deliberately excluded from the model development. Finally the model was implemented within a Geographical Information System (GIS) to aid usability.

A shortcoming of the model was that during the experimental field work, the majority of train speeds recorded were between 75 km/h and 130 km/h. Although a small number were higher, a maximum speed of 200 km/h was recorded, which is lower than the velocities typically experienced on commercial high speed rail lines. Therefore the relationships developed in this work were only valid for lower speed trains. Additionally, the curve fitting used in this work was linear, thus possibly over simplifying the relationship between model variables and predicted r.m.s. (root mean square) values.

The Federal Railroad Administration [10] and Rossi et al. [27] also proposed empirical models for preliminary study purposes. Rossi et al. [27] proposed a model based upon making assumptions about wave propagation and [10] was constructed solely using field experiment results. The Federal Railroad Administration approach [10] was based on a collection of ground-borne velocity and acceleration recordings from European railway sites. These results were converted to 1/3 octave bands [26] and statistically analysed to determine correlations between a discrete number of track setups. The resulting model approximated vibration levels on a velocity log scale and was straightforward to use. This ease of use meant that the model gained wide acceptance and is commonly used on commercial projects.

A limitation of [10] was that the soil properties at each site were not determined [12], meaning the model ignored the effect of soil conditions on wave propagation. Therefore, factors such as Rayleigh wave speed were not considered in the vibration prediction. The only exception to this was if the track was characterised as resting on soil conditions that 'promoted efficient vibration' such as rock. This omission is highly relevant because soil properties have been shown to contribute significantly to the levels of ground vibrations generated by railway tracks, particularly in the free field ([18,22,1]). Thus, ignoring soil properties is likely to reduce the accuracy of a prediction model.

Another drawback of [10] was that it could only be used to predict VdB (vibration decibels) values. Although VdB is acceptable for use with a few isolated vibration guidelines (particularly in America) there are many countries where this metric is not compatible with national standards.

This paper uses a combination of numerical modelling and machine learning to overcome the shortcomings of the Federal Railroad Administration approach [10]. First a numerical model is presented which is capable of predicting railway vibration levels with accuracy. Next some considerations for constructing a new model (called 'ScopeRail') based on previously calculated synthetic vibration records are discussed. Finally, the model is tested against vibration levels from four high speed lines and is shown to have high prediction abilities for two international metrics. The new tool forms part of a suite of prediction models under development at Heriot Watt University.

2. Numerical approach

The newly proposed vibration prediction tool ('ScopeRail') was developed using a statistical approach, which was in principle, similar to [10]. A key difference was that instead of using vibration levels recorded during experimental field trials for the statistical analysis, vibration time histories were generated using a high accuracy numerical model. The advantage of this approach was that the soil properties were fully known for each train passage and thus could be included in the statistical analysis. Furthermore, the effect of a wide range of soil properties on

vibration levels could be analysed without performing physical investigations at a large number of test sites, each with diverse soil characteristics. The general principle behind the model development process is outlined in Fig. 1.

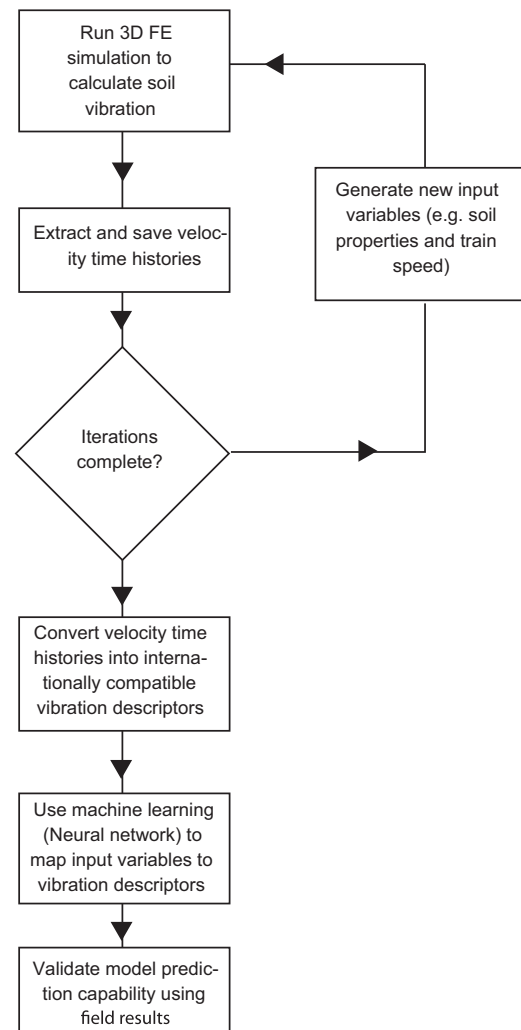


Fig. 1. ScopeRail model development.

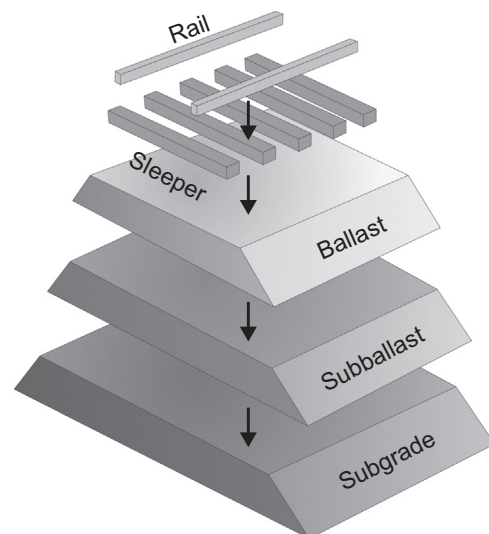


Fig. 2. Track layout.

2.1. Detailed vibration prediction model development

To populate a database of ground vibration records, a 3D finite element model was developed capable of modelling high speed rail vibrations. The model consisted of an elastic, fully coupled train, track and soil model.

The track was modelled in a configuration similar to that found on many European high speed lines. It consisted of a continuously welded rail supported by concrete sleepers laid at 0.65 m centres. The sleepers were then supported by a 0.3 m layer of ballast, a

0.2 m layer of subballast and finally a 0.3 m layer of subgrade. The arrangement is shown in Fig. 2. The rail was meshed using 0.1 m beam elements whereas all other track components were meshed using 0.2 m solid square brick elements. The track length in the direction of train passage was 60 m and the ends of the ballast, subballast and subgrade were terminated using infinite elements.

The soil was modelled as a stratified halfspace with four sides truncated by an absorbing boundary condition (infinite elements) to prevent spurious reflections. The remaining two sides were bounded by a symmetry boundary condition and a free surface, respectively. A sample mesh of the fully coupled soil and track model is shown in Fig. 3.

The vehicle was modelled using a lumped mass multi-body approach (Fig. 4). The cars, bogies and wheels were connected using springs and dashpots to model the vehicle suspension characteristics (Table 1). Each wheel was coupled to the rail using a non-linear Hertzian contact spring, as described by:

$$F_{wr} = k_H(u_w - u_r - r)^{1.5}, \text{ if } u_w - (u_r + r) < 0$$

$$F_{wr} = 0, \text{ if } u_w - (u_r + r) > 0 \tag{1}$$

where ‘ F_{wr} ’ was the force generated at the wheel and rail interface, ‘ u_w ’ was the wheel displacement, ‘ u_r ’ was the rail displacement and ‘ r ’ was the rail irregularity. This formulation allowed for the contact force to be a function of the wheel and rail positions relative to each other, rather than a constant point load. For this study, due to the unpredictable nature of rail irregularity and the desire to reduce the number of input variables, the rail was assumed to be perfectly smooth (i.e. no irregularity, $r=0$). This assumption was valid, particularly for high speed rail lines, where track standards require that rail unevenness is maintained below a very low threshold.

It should also be noted that only half of all three model components (track, soil and vehicle) were modelled due to the symmetry associated with the physical problem. Analysis was computed via the commercial finite element package ABAQUS, using a dynamic explicit central differencing scheme. The advantage of this approach allowed for the complex track geometries to be modelled in detail, and for the calculations to be spread across multiple processors in a straightforward manner. Additional details related to the model development are available in [6,5]. Visualisations of the final model, showing the displacements of the soil and track as the train traverses the domain are shown in Figs. 6 and 7.

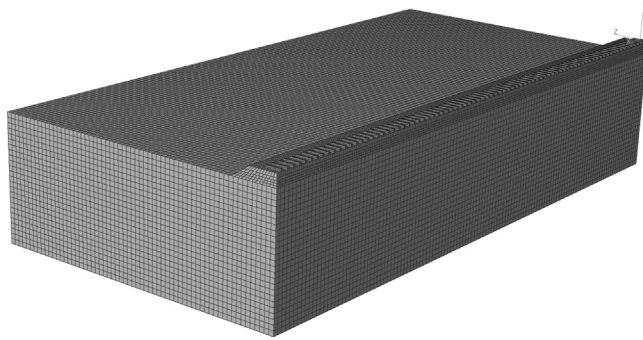


Fig. 3. Finite element layout.

Table 1
Thalys properties.

	Thalys		
	Bogie Y230A (Driving car)	Bogie Y237A (Passenger car)	Bogie Y237B (Side car)
Half-car body mass (kg)	26,721	14,250	20,426
Bogie mass (kg)	3261	1400	8156
Wheelset mass (kg)	2009	2050	2009
Primary suspension stiffness (MN/m)	2.09	1.63	2.09
Primary suspension damping (kN s/m)	40	40	40
Secondary suspension stiffness (MN/m)	2.45	0.93	2.45
Secondary suspension stiffness (kN s/m)	40	40	40

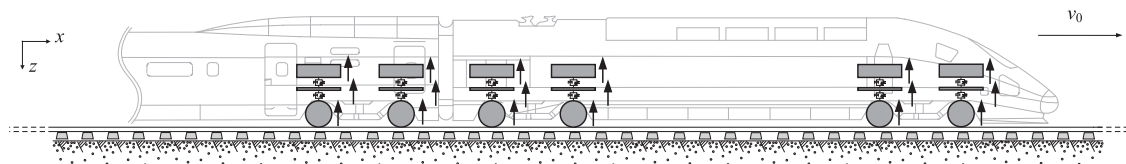


Fig. 4. Thalys carriage layout.



Fig. 5. Left: Field work equipment, Right: Test site setup.

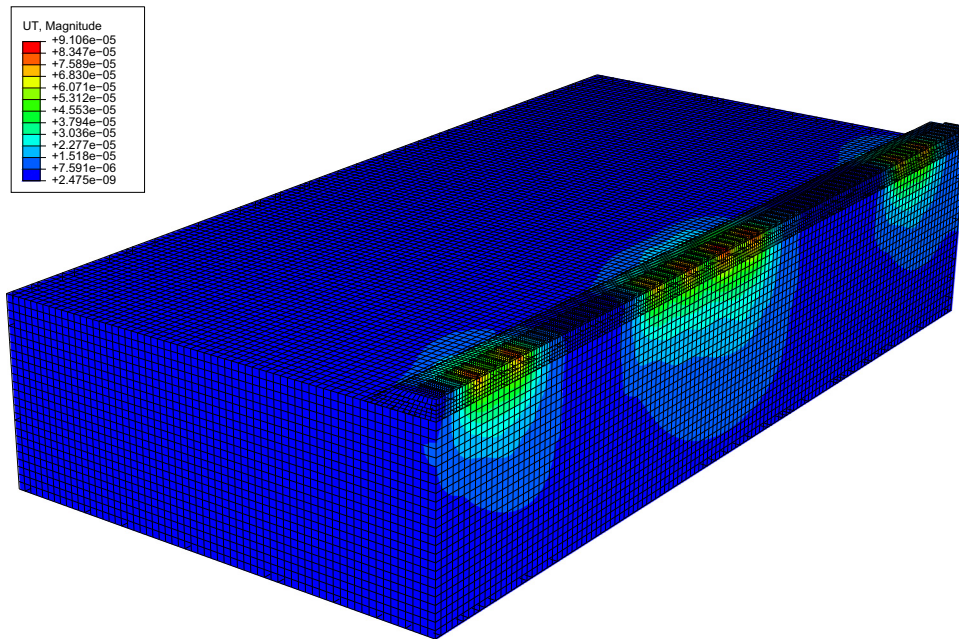


Fig. 6. Numerical visualisation of the passage of a high speed train.

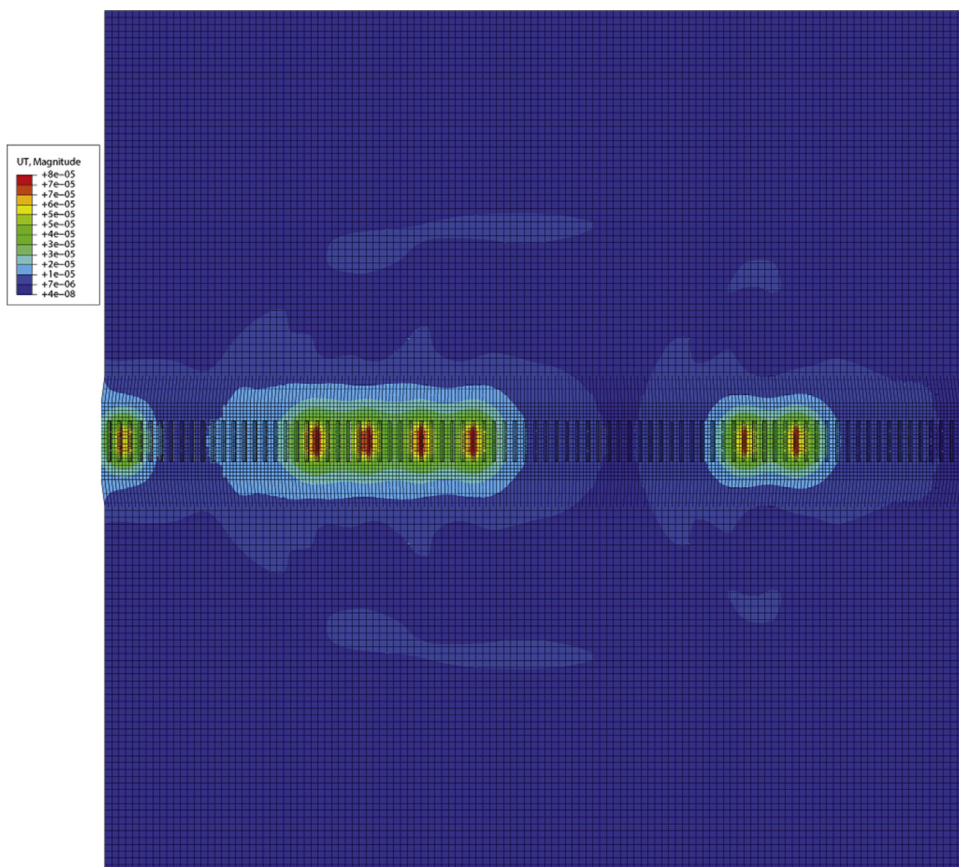


Fig. 7. Birdseye view visualisation of the passage of a high speed train (distance of travel: right to left).

3. Model validation

3.1. Field work

Experimental work was undertaken for the purpose of determining whether the numerical model could produce vibration predictions

with sufficient accuracy to allow it to be used for the machine learning approach. A test site was chosen in Belgium on the Brussels to Paris line, which was subject to the passage of Thalys, Eurostar and TGV locomotives ([17]). Vertical vibration levels were measured using 4.5 Hz geophones (mounted on 150 mm spikes) placed at distances between 7 m and 100 m from the track (Fig. 5). The signals were

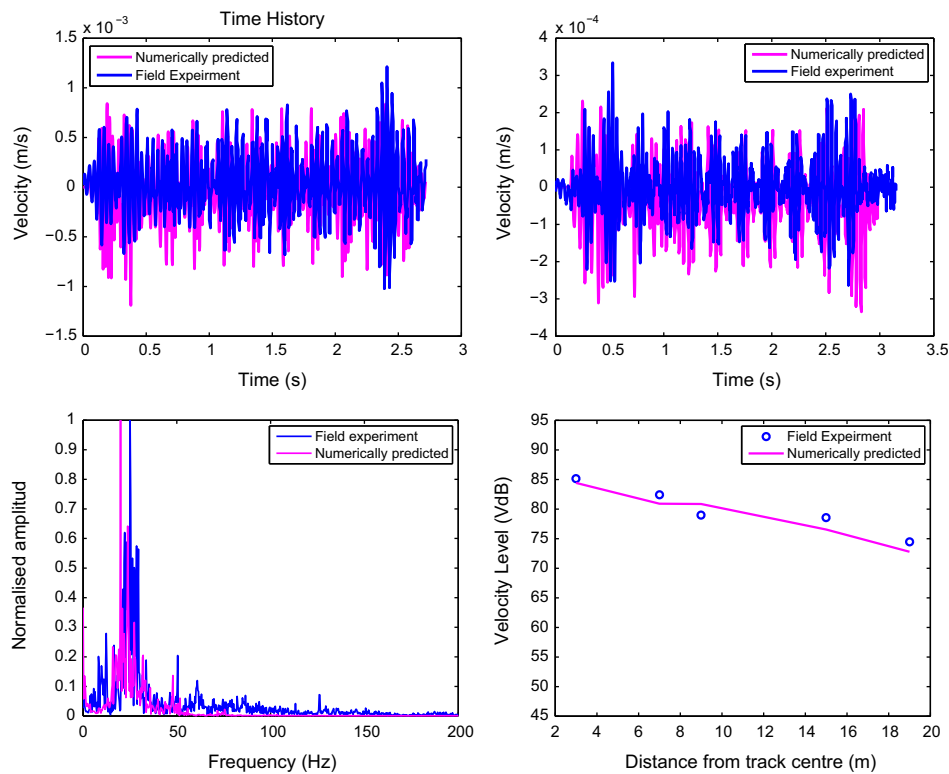


Fig. 8. Model validation, (a) Top left: vertical velocity time history 7 m from track centre. (b) Top right: vertical velocity time history 19 m from track centre. (c) Lower left: Normalised vertical velocity frequency content at 7 m from track. (d) Lower right: VdB variation with distance from track.

digitally converted using a 24 channel Geode exploration seismograph and recorded using a Panasonic Toughbook CF-19 (Fig. 5). For each train passage the train speed was determined during post-processing using an efficient and robust calculation method based on dominant frequency analysis [16].

To calculate the underlying soil properties a multi-channel analysis of surface waves (MASW) technique was used. First, a 12 lb instrumented hammer was used to excite an impact plate resting on the soil surface and the resulting velocity time histories were recorded using geophones placed at 1 m spacings. The response from all 24 geophones was then post-processed to construct a dispersion curve, which was then inverted to obtain an approximation for the underlying soil properties. Material damping was calculated by constructing a 2D soil finite element model in combination with a curve fitting approach to approximate a single damping coefficient for the 1D soil profile.

It is seen from Fig. 8 that the numerical model performed well. At both 7 m and 19 m from the track the model was able to accurately predict the timing, magnitude and shape of the velocity time history. Similarly, the frequency content was well resolved with the dominant frequencies being identified to be located around 30 Hz. The VdB results also showed a high correlation between predicted and experimental results. The predicted value at each location was within approximately 2 dB of the experimental value.

4. Parameter sensitivity analysis

There are a wide range of physical properties that can affect vibration levels from high speed trains. To model each of these numerically would require a separate variable to be included to describe each property. This is impractical when using machine learning approaches because as the number of variables increases, the number of data points (i.e. numerically generated vibration records) required to accurately map inputs and outputs grows

exponentially. Therefore it is important to limit the number of model variables. To do this the least influential parameters were identified. They were then removed and only the most influential ones were kept.

4.1. Soil property sensitivity analysis

The purpose of a vibration scoping tool is to provide high speed rail planners (with no prior geotechnical experience) with a method to instantaneously assess vibration levels. Therefore it is important that existing elementary borehole information (or other geotechnical information) can be easily translated into input variables for the model. Therefore, to aid this it was important that only a minimal number of input variables would be required to use the new model. Thus, a sensitivity analysis was undertaken to determine the effect each FE soil property had on vibration propagation. This way, it was possible to quantify the least influential parameters and remove them from the analysis.

Density, Poisson's ratio and Young's modulus play different roles in describing wave propagation. Consequently the sensitivity of wave propagation to each parameter is different. For the range of soil parameters typically found in-situ, the effect of each parameter on peak particle velocity (PPV) levels was tested.

For each test the model properties were kept constant, unless otherwise stated, with Young's modulus=100 MPa, density=2000 kg/m³, Poisson's ratio=0.3 and material damping ratio=0%. Between five and seven simulations were performed to investigate the sensitivity of each parameter on PPV. The first simulation was performed using a parameter at the lower end of that for a typical soil and the second was performed using a parameter at the upper end of that for a typical soil. The excitation was of the form of the first derivative of a Gaussian and the PPV results were normalised with respect to the PPV value calculated at 0.5 m from the source, with respect to the lower value material parameter under investigation.

To compute the soil response due to each variation in material properties, a two dimensional, explicit finite difference time domain (FDTD) method was used. This approach was chosen because the number of cells required to resolve the 10 Hz propagating wave was dependent on the soil material properties. Therefore each change in material properties required a unique mesh. Using the FDTD method allowed the mesh to be updated automatically at the start of each iteration, thus ensuring that the wave propagation was correctly simulated.

The FDTD model was implemented using a rotated staggered grid stencil [28] to model the stress (T_{xx} , T_{zz} , T_{xz}) and velocity components (V_x , V_z) within the grid. The model layout and discretisation is shown in Fig. 9. The free surface boundary was achieved by explicitly assigning all grid points above the surface with very low shear wave velocities and densities. The explicit integration scheme was second order in space and time to ensure continuity at the surface. The left hand side was defined using a symmetry boundary condition to reduce the problem domain by 50%, and the other two boundaries were bound by a series of perfectly matched layers (PML [9]). These PML layers were implemented using second order stretching functions [11] to optimise their ability to absorb outgoing waves.

Fig. 10 shows the effect of density on normalised PPV with increasing distance from the excitation point. The change in PPV between 1300 kg/m^3 and 2300 kg/m^3 is relatively constant at all observation points. A similar trend is observed for Poisson's ratio which is also insensitive to changes between 0.2 and 0.4. Despite this, as distance increases, the vibration level generated by the lowest Poisson's ratio value (0.2) starts to increase in comparison to the highest value (0.4).

Young's modulus exhibits much different characteristics in comparison to Poisson's ratio and density (Fig. 10). The difference between the maximum and minimum Young's modulus values is much more significant which is true for all distances however the discrepancy changes from approximately 90% at a distance of 0.5 m to approximately 65% at 7.5 m. It was also noticed that as Young's modulus increased, the decrease in PPV was not linear. Instead, the PPV decrease followed a more exponential relationship.

A comparison between the variance in PPV values generated by changes in each material property is also shown in Fig. 10. It is clear that for typical soil properties, the Young's modulus has a much greater influence on vibration levels than density or Poisson's ratio. Approximately, the variations in Young's modulus,

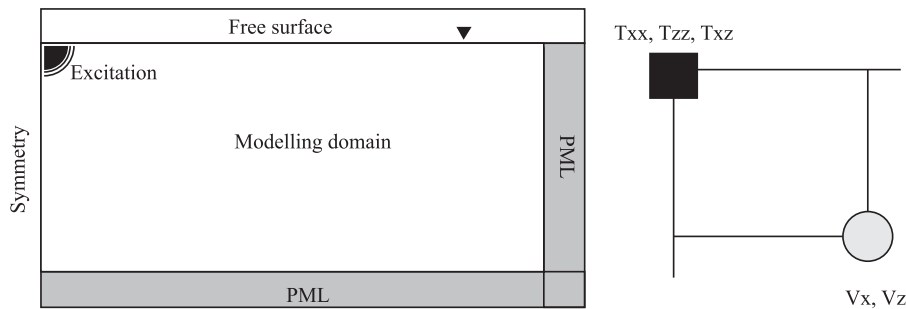


Fig. 9. Left: FDTD model schematic, Right: Rotated staggered grid stencil.

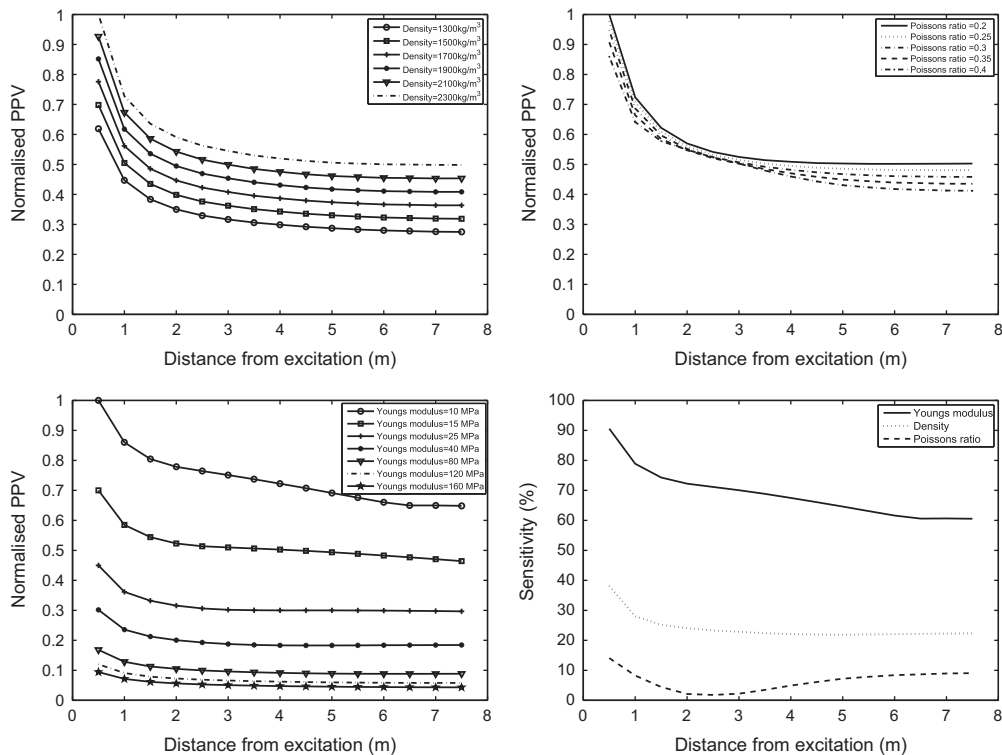


Fig. 10. PPV sensitivity (a) Top left: density, (b) Top right: Poisson's ratio, (c) Bottom left: Young's modulus, (d) Bottom right: Overall parameter sensitivity).

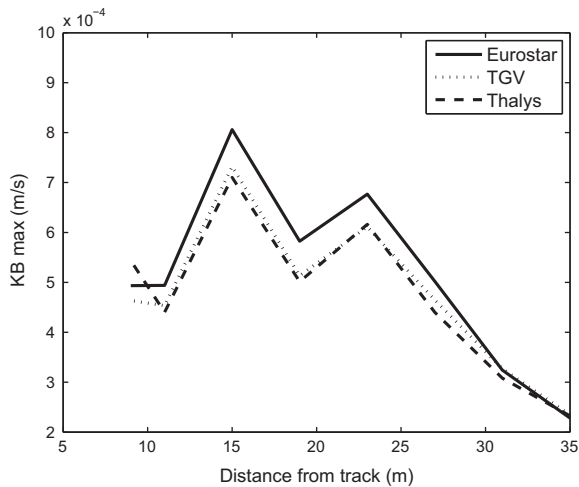


Fig. 11. The effect of train type on KB_{max} (train speeds, 300 km/h).

density and Poisson's ratio can be seen to introduce errors of 65%, 10% and 25% into the PPV calculation. Therefore, for the purpose of reducing the number of input variables required for the empirical model, it was concluded that it would be sufficient to remove Poisson's ratio and density as potential variables. Thus, only Young's modulus was used to describe the soil properties within the model.

4.2. Train type sensitivity analysis

As part of the field work undertaken in Belgium, three of the most common steel wheeled high speed train types found in Europe were recorded (Eurostar, TGV and Thalys). To determine the effect of each train type on vibration levels, the recorded signals were compared. All three train passages were of similar speed and recorded at the same test site, on the same day. Although the vibration levels (both PPV and KB) at all distances were found to be slightly elevated for Eurostar passages, the overall responses were similar for all trains (Fig. 11). Therefore it was concluded that train type had a minimal impact and that a train type variable was not required to develop the ScopeRail. Instead all train passages could be performed using a Thalys train.

5. Machine learning approach

A neural network (NN) approach was chosen as the learning method to develop ScopeRail due its non-linear regression ability. NN techniques have been used successfully in wave propagation modelling to predict vibration levels from blasting in the mining industry [24], to investigate the performance of 2D trenches to isolate railway vibration [13], to relate railway track geometry to vehicle performance [21] and to estimate shear wave velocities of soils from geophysical tests [25].

A 'back propagation', multilayer perceptron neural network architecture was used to map the inputs to outputs (Fig. 12). This meant that there was a hidden layer between the input and output nodes with several hidden nodes, and that errors were fed back through the network. The training patterns were first propagated forward through this network structure and compared against the output targets. The error was then propagated back through the network and the node weightings updated. The newly predicted outputs were then compared against the output targets to determine the error.

To construct the database of output values, the ABAQUS model was computed for 360 permutations of the input parameters, and

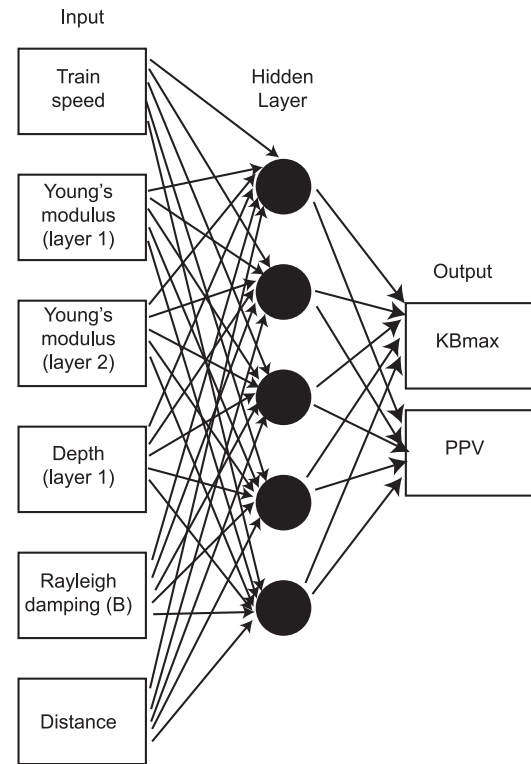


Fig. 12. Homogenous ANN model schematic.

2700 data points were used in the creation of the network. For each simulation a Thalys high speed train was chosen as the excitation model and rail irregularity was ignored. For each simulation, the computational run time for a full Thalys trainset with 10 carriages (three seconds of modelling time) took approximately 50 h. To reduce computational time the excitation model was reduced to a single driving carriage with four wheels. This reduced the run times to 10 h. Comparisons were made between the PPV and KB results obtained from each model (single and full trainset) and the discrepancy was found to be small (4.6%) meaning the four wheel model provided a reasonable approximation of a full Thalys trainset.

The range of values for each input parameter was chosen carefully to cover a wide range of parameters likely to be found in real life. Two soil layers were used to allow for more detailed soil input values to be used in the model in comparison to a homogenous half-space. It was proposed that a two layer model would help prediction accuracy significantly, especially in cases where there was a strong contrast in soil stiffness below the ground surface. To enable fast development of two layer ABAQUS models each with different layer depths and material properties, a MATLAB code was developed. This code was used to directly edit a generic ABAQUS input file and modify the required FE parameters.

5.1. Soil layer mapping

The scoping model was only capable computing a discrete number of input soil layers (2 layers), however many physical soil profiles consist of a greater number of layers. Therefore, to enable the model to be used at any test site, the soil property input information was converted into a 2 layer soil. This translation was performed using a straightforward thickness weight average technique as outlined in [4]:

$$E_{eq} = \frac{\sum H_i E_i}{\sum H_i} \quad (2)$$

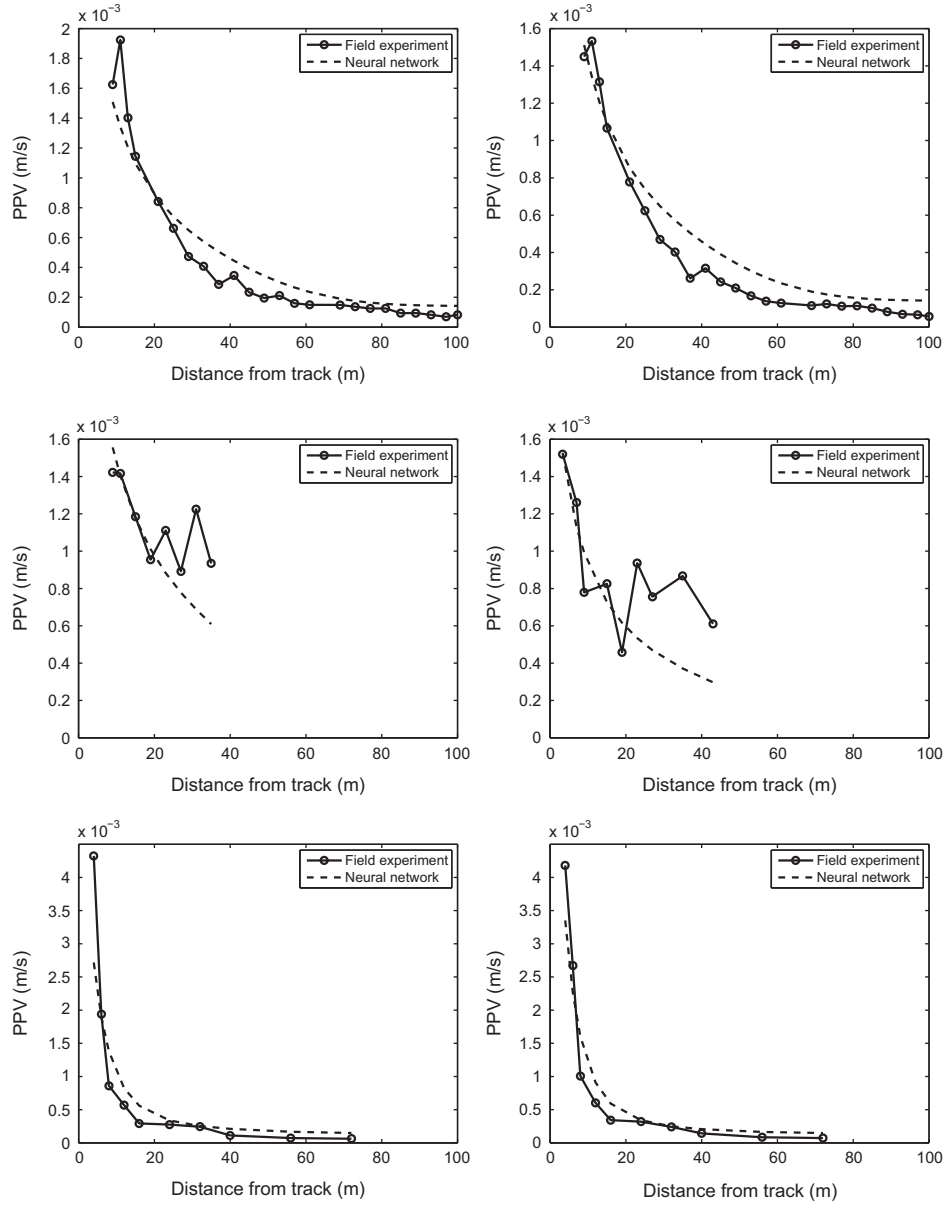


Fig. 13. PPV results, (a) Top left: Mons 2012, 291 km/h (b) Top right: Mons 2012, 294 km/h, (c) Middle left: HS1 2012, 270 km/h, (d) Middle right: Mons 2005, 265 km/h, (e) Bottom left: Degrande 2001, 271 km/h, (f) Bottom right: Degrande 2001, 300 km/h.

where E_{eq} =equivalent Young's modulus, H_i =each layer thickness and E_i =Young's modulus of each layer.

5.2. Vibration descriptors

Each numerical simulation generated a series of velocity time histories, each corresponding to a different distance from the railway track. Rather than attempt to use the neural network approach to predict each time history, it was used to predict two commonly used vibration metrics. The first metric was peak particle velocity (PPV) which is typically used for analysing the effect of vibrations on structures. The second metric was $KB_{F,max}$ which is more commonly used to assess the impact of vibrations on humans. It can be seen that PPV is a measure of the instantaneous maximum amplitude of vibration, whereas $KB_{F,max}$, defined as the maximum of KB_F , accounts also for the duration of the signal.

$$PPV = \max |\nu(t)| \quad (3)$$

$$KB_F(t) = \sqrt{\frac{1}{\tau} \int_0^t KB^2(\xi) e^{-\frac{t-\xi}{\tau}} d\xi} \quad (4)$$

where $\tau=0.125$ s. It is based upon the calculation of a weighted velocity signal $KB(t)$, defined by the analytical filter:

$$H_{KB}(f) = \frac{1}{\sqrt{1 + \left(\frac{5.6}{f}\right)^2}} \quad (5)$$

6. Numerical results

6.1. Test site descriptions

To ensure that ScopeRail was capable of predicting vibration levels for a variety of test sites and that it had not been over-fitted to the test site that was used to validate the FE model, it was validated using four different sets of experimental results.

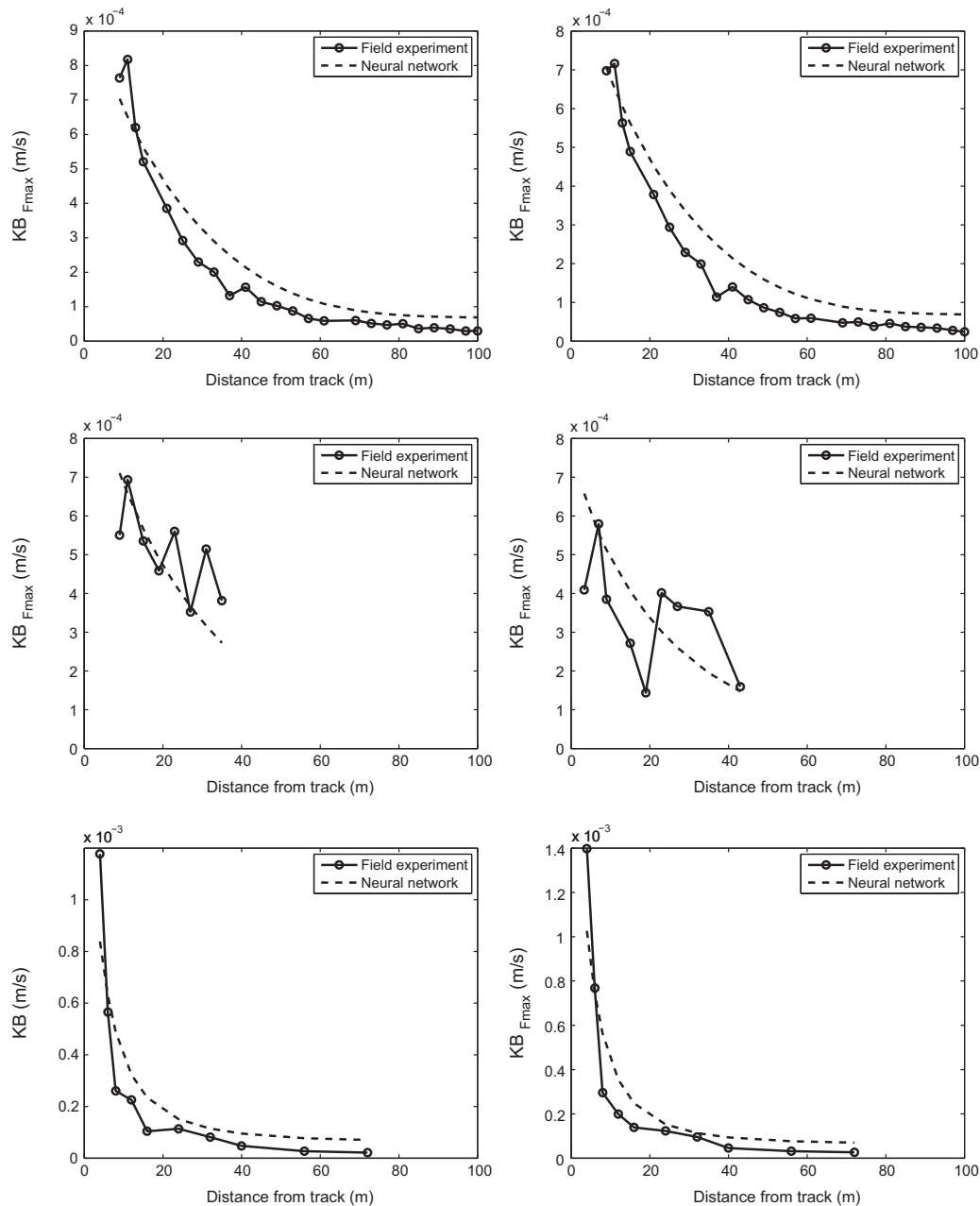


Fig. 14. $KB_{F,max}$ results, (a) Top left: Mons 2012, 291 km/h (b) Top right: Mons 2012, 294 km/h, (c) Middle left: HS1 2012, 270 km/h, (d) Middle right: Mons 2005, 265 km/h, (e) Bottom left: Degrande 2001, 271 km/h, (f) Bottom right: Degrande 2001, 300 km/h.

The first set of results were the aforementioned ones recorded in Belgium in 2012 [17]. These were then denoted as 'Mons 2012'. The second set of results were recorded in England on the London to Paris high speed line, using identical experimental equipment to that for Mons 2012, however only to a distance of 35 m. These were denoted 'HS1 2012'. The third set of results (Mons 2005) were recorded in Belgium in 2005 using geophones and a more detailed description of the test setup can be found in [20]. Lastly, the final set of results were also recorded in Belgium and denoted 'Degrande 2001'. Vibration levels were sampled using accelerometers and then converted to velocity time histories. A more detailed experimental description is found in [8].

6.2. PPV prediction analysis

Fig. 13 shows a comparison between the new tool and the experimental results. The results from Mons 2012 are plotted

up to a distance of 100 m from the track whereas the results from HS1, Mons 2005 and Degrande 2001 are plotted up to distance of 35 m, 43 m and 72 m, respectively. Each of these distances was a function of the maximum geophone offset used during experimental testing. For the Mons 2012 and Degrande 2001 test sites the decrease in PPV levels broadly followed the expected inverse squared relationship. This was particularly clear for the Degrande results due to the low offset of the closest receiver to the track (4 m) which experienced high velocity levels. For the HS1 and Mons 2005 test sites the variation of PPV with distance was less uniform, possibly due to the lack of experimental data or localised soil artefacts.

It was found that ScopeRail replicated the results from Mons 2012 and Degrande 2001 with high accuracy, with only minor discrepancies found. This was true for all distances from the track. Considering HS1 and Mons 2005 test sites, it also

performed well and predicted a reasonable 'best fit' curve between the data points. Despite this, it was unable to predict the aforementioned and unaccounted for, local increases in PPV.

6.3. $KB_{F,max}$ prediction analysis

Fig. 14 shows comparisons between the scoping model and the experimental results recorded at the same four test sites as described in Section 6.2. Similarly to the PPV results, the model is capable of predicting the vibration levels at Mons 2012 with accuracy, with all distances having only minor discrepancies. The magnitude of the HS1 2012 and Mons 2005 results is predicted slightly better for $KB_{F,max}$ than PPV, with the numerical results once again passing through the experimental ones with a strong correlation. Lastly, the predicted Degrande 2001 results have a high fit with the experimental ones for all distances. Furthermore, the exponential decrease in vibration levels is resolved well as the distance from the track increases.

7. Discussion

ScopeRail was found to offer strong prediction performance for all test sites. Prediction accuracy was highest for the Mons 2012 and Degrande 2001 test sites because at these locations the distribution of vibration levels with distances was relatively uniform, thus making them more straightforward to simulate numerically. The HS1 2012 and Mons 2005 data sets contained vibration levels with a greater number of unexpected local increases in vibration level. Therefore they were more challenging for a numerical model to predict, however the scoping model was able to generate results that corresponded well to a best-fit line through the results. Therefore it was concluded that the new model offered strong prediction performance for all experimental sites tested. This high accuracy may offer cost savings on high speed rail projects because fewer regions will suffer from over-predicted vibration levels. Despite this, for regions where vibration levels are found to exceed national/international standards, it is recommended that the follow-up study uses a more detailed modelling approach.

8. Conclusions

A new scoping railway vibration prediction model ('ScopeRail') was developed capable of predicting three international vibration metrics in the presence of layered soils. The development of the new model was outlined starting with the description of a high accuracy 3D finite element model. This 3D model was used to populate a database of vibration records, which was then used to establish relationships between key railway variables using a machine learning approach.

The resulting empirical model had zero run times and was capable of predicting two internationally recognised vibration assessment metrics. Model performance was tested against field results collected at four high speed rail test sites and it was found to have high accuracy prediction capabilities for all.

This increase in accuracy can potentially reduce the volume of detailed vibration analyses required for a new line. This has the potential to minimise costly in-depth studies in the form of field experiments or large numerical models. Therefore the use of the new tool can result in cost savings.

Acknowledgements

The authors wish to thank the University of Edinburgh, the University of Mons and Heriot Watt University for the support and resources provided for the undertaking of this research. Additionally, the funding provided by Engineering and Physical Sciences Research Council (EP/H029397/1) and the Natural Environment Research Council is also greatly appreciated, without which, this research could not have been undertaken.

References

- [1] Auersch, L. (2008). The influence of the soil on track dynamics and ground-borne vibration. In noise and vibration mitigation for rail transportation systems. In: Proceedings of the ninth international workshop on railway noise, T Maeda, P-E Gautier, CE Hanson, B Hemsworth, JT Nelson, B Schulte-Werning, D Thompson, and P de Vos, editors, vol. 99 (pp. 122–128). Munich, Germany.
- [2] Bahrekazemi, M. (2004). Train-induced ground vibration and its prediction. PhD thesis. Stockholm University.
- [3] Beskos D, Dasgupta B, Vardoulakis I. Vibration isolation using open and filled trenches. Part 1: 2D homogeneous soil. *Comput Mech* 1986;1:43–63.
- [4] Brahma, P, Mukherjee, S. (2010). A realistic way to obtain equivalent Young's modulus of layered soil. In: Indian geotechnical conference. Bombay, India. p. 305–308.
- [5] Connolly D, Giannopoulos A, Fan W, Woodward PK, Forde MC. Optimising low acoustic impedance back-fill material wave barrier dimensions to shield structures from ground borne high speed rail vibrations. *Constr Build Mater* 2013;44:557–64, <http://dx.doi.org/10.1016/j.conbuildmat.2013.03.034>.
- [6] Connolly D, Giannopoulos A, Forde M. Numerical modelling of ground borne vibrations from high speed rail lines on embankments. *Int J Soil Dyn Earthquake Eng* 2013;46:13–9, <http://dx.doi.org/10.1016/j.soildyn.2012.12.003>.
- [8] Degrande G, Schillemans L. Free field vibrations during the passage of a Thalys high-speed train at variable speed. *J Sound Vib* 2001;247(1):131–44, <http://dx.doi.org/10.1006/jsvi.2001.3718>.
- [9] Drossaert FH, Giannopoulos A. A nonsplit complex frequency-shifted PML based on recursive integration for FDTD modeling of elastic waves. *Geophysics* 2007;72(2):T9, <http://dx.doi.org/10.1190/1.2424888>.
- [10] Federal Railroad Administration. (2012). High-speed ground transportation noise and vibration impact assessment. U.S. Department of Transportation (pp. 1–248).
- [11] Giannopoulos, A, Melling, S, Connolly, D. (2012). A second order PML implementation for FDTD seismic modelling. In: near surface geoscience 2012–18th European meeting of environmental and engineering geophysics.
- [12] Harris, Miller, Hanson. (1996). Summary of European high speed rail noise and vibration measurements (HMMH Report No. 293630-2). p. 1–158.
- [13] Hung C, Ni S. Using multiple neural networks to estimate the screening effect of surface waves by in-filled trenches. *Comput Geotech* 2007;34(5):397–409, <http://dx.doi.org/10.1016/j.compgeo.2007.06.005>.
- [14] Kattis S, Polyzos D, Beskos D. Vibration isolation by a row of piles using a 3-D frequency domain BEM. *Int J Numer Methods Eng* 1999;728:713–28 (February).
- [15] Kattis S, Polyzos D, Beskos D. Modelling of pile wave barriers by effective trenches and their screening effectiveness. *Int J Soil Dyn Earthquake Eng* 1999;18(1):1–10, [http://dx.doi.org/10.1016/S0267-7261\(98\)00032-3](http://dx.doi.org/10.1016/S0267-7261(98)00032-3).
- [16] Kouroussis, G, Connolly, D, Forde, M, Verlinden, O. (2013a). Train speed calculation using ground vibrations. *J Rail Rapid Transit*.
- [17] Kouroussis, G, Connolly, D, Forde, M, Verlinden, O. (2013b). An experimental study of embankment conditions on high-speed railway ground vibrations. In: International congress on sound and vibration. Bangkok, Thailand. p. 1–8.
- [18] Kouroussis G, Conti C, Verlinden O. Investigating the influence of soil properties on railway traffic vibration using a numerical model. *Veh Syst Dyn* 2013;51(3):421–2, <http://dx.doi.org/10.1080/00423114.2012.734627>.
- [20] Kouroussis G, Verlinden O, Conti C. Free field vibrations caused by high-speed lines: measurement and time domain simulation. *Int J Soil Dyn Earthquake Eng* 2011;31(4):692–707, <http://dx.doi.org/10.1016/j.soildyn.2010.11.012>.
- [21] Li, D, Meddah, a, Hass, K, Kalay, S. (2006). Relating track geometry to vehicle performance using neural network approach. *Proc Inst Mech Eng Part F J Rail Rapid Transit*, 220(3), 273–281, <http://dx.doi.org/10.1243/09544097JRR39>.
- [22] Lombaert G, Degrande G, Clouteau D. The influence of the soil stratification on free field traffic-induced vibrations. *Arch Appl Mech* 2001;71(10):661–78, <http://dx.doi.org/10.1007/s004190100174>.
- [23] Madhus C, Bessason C, Harvik L. Prediction model for low frequency vibration from high speed railways on soft ground. *J Sound Vib* 1996;193(1):195–203, <http://dx.doi.org/10.1006/jsvi.1996.0259>.
- [24] Monjezi M, Ghafurikalajahi M, Bahrami a. Prediction of blast-induced ground vibration using artificial neural networks. *Tunnelling Underground Space Technol* 2011;26(1):46–50, <http://dx.doi.org/10.1016/j.tust.2010.05.002>.
- [25] Nazari, S, Saljooghi, S, Shahbazi, MM, Akbari, HR. (2010). Application of artificial neural networks in solving inversion problem of surface wave method on pavements. In: Second international conference on engineering optimization. Lisbon, Portugal. p. 1–8.

- [26] Nelson J, Saurenman H. A prediction procedure for rail transportation groundborne noise and vibration. *Transp Res Rec: Journal of the Transportation Research Board* 1987;1143:26–35.
- [27] Rossi F, Nicolini A. A simple model to predict train-induced vibration: theoretical formulation and experimental validation. *Environ Impact Assess Rev* 2003;23(3):305–22, [http://dx.doi.org/10.1016/S0195-9255\(03\)00005-2](http://dx.doi.org/10.1016/S0195-9255(03)00005-2).
- [28] Saenger E, Gold N, Shapiro S. Modeling the propagation of elastic waves using a modified finite-difference grid. *Wave Motion* 2000;31:77–92, [http://dx.doi.org/10.1016/S0165-2125\(99\)00023-2](http://dx.doi.org/10.1016/S0165-2125(99)00023-2).